Developments in Marine Corrosion

Edited by

S.A. Campbell, N. Campbell and F.C. Walsh

Applied Electrochemistry Group, University of Portsmouth, Portsmouth, UK

RS•C
ROYAL SOCIETY OF CHEMISTRY

3. ELECTROCHEMICAL AND ATOMIC FORCE MICROSCOPY STUDIES OF A COPPER NICKEL ALLOY IN SULPHIDE-CONTAMINATED SODIUM CHLORIDE SOLUTIONS

G.J.W. Radford[a], F.C. Walsh[a], J. R Smith[a], C.D.S. Tuck[b] and S.A. Campbell[a],

[a]*Applied Electrochemistry Group, University of Portsmouth, St. Michael's Building, White Swan Road, Portsmouth, PO1 2DT (UK).* [b]*Meighs Ltd., Langley Alloys Division, Campbell Road, Stoke-on-Trent, Staffs, ST4 4ER (UK).*

Abstract

The electrochemical behaviour of copper and a high strength 70/20 copper nickel alloy, MARINEL™ (MARINEL™ is a registered trade make of Langley Alloys Ltd.), was investigated in sulphide contaminated and uncontaminated sodium chloride solutions (3.0%) at 293 K. Cathodic polarisation curves for the oxygen reduction reaction exhibited a well-defined plateau region between -650 and -1150 mV (*vs.*SCE) prior to hydrogen evolution. In the presence of 5 ppm sulphide ions, an additional plateau region between -480 and -850 mV (*vs.* SCE) is observed which is attributable to the production of hydrogen peroxide. This plateau is more prominent on copper than on the high strength alloy. The diffusion coefficient for dissolved oxygen was determined in the presence and absence of sulphide. Oxygen reduction was similar on copper nickel and copper leading to diffusion coefficients of 1.50×10^{-5} and 1.44×10^{-5} cm^2 s^{-1} respectively. In the presence of 5 ppm sodium sulphide, the diffusion coefficient values were reduced to 1.35×10^{-5} and 1.24×10^{-5} cm^2 s^{-1}, respectively. Atomic force microscopy investigations of the initiation of corrosion and the influence of passive layers on the corrosion reaction confirmed that film formation was rapid. In the presence of sulphide ions, particle size increases from 68 to 300 nm in diameter were observed for both surface films but the particle heights were of similar dimensions, 6 nm. The increase in particle size for films produced in sulphide

contaminated solutions would be expected to influence film porosity and hence the corrosion resistance.

Symbols	**Units**
I_L = Limiting current	A
n = Number of electrons involved in the electrode process	
F = Faraday constant	A s mol^{-1}
ω = Rotation rate of the disc	rad s^{-1}
ν = Kinematic viscosity of the electrolyte	cm^2 s^{-1}
c_B = Bulk concentration of dissolved oxygen	mol cm^{-3}
D = Diffusion coefficient of dissolved oxygen	cm^2 s^{-1}
A = Area of electrode	cm^2

1. INTRODUCTION

Copper and its alloys are used extensively as marine and engineering structural materials due to their excellent corrosion resistance and anti-fouling properties which result from their naturally occurring, protective corrosion products. Over the last 20 years, there have been rapid developments in their use as coatings and fasteners. Copper alloys, particularly cupro-nickels, are used as cladding materials in antifouling applications and the high strength, age hardening copper nickels have been widely used for offshore bolting applications[1].

It is generally accepted that the open circuit corrosion of freshly polished copper alloys involves the reduction of oxygen and the production of cuprous ions[2],

$$O_{2(g)} + 2H_2O_{(l)} + 4e^- \rightarrow 4OH^-_{(aq)} \quad \text{(cathodic reaction)} \qquad (1)$$

$$Cu_{(s)} \rightarrow Cu^+_{(aq)} + e^- \quad \text{(anodic reaction)} \qquad (2)$$

followed by the formation of a copper(I)-chloro complex,

$$Cu^{+}(aq) + 2Cl^{-}(aq) \rightarrow CuCl_2^{-}(aq) \quad (3)$$

Cuprous oxide is widely acknowledged to be the initial product of corrosion[3-6],

$$2CuCl_2^{-}(aq) + 2OH^{-}(aq) \rightarrow Cu_2O(s) + H_2O(l) + 4Cl^{-}(aq) \quad (4)$$

and is generally doped with alloying elements which can render it more protective than copper[7]. The presence of nickel and iron as minor components in the lattice of the corrosion layer on copper nickels decreases its defect number, thus increasing its passivating power[4].

After prolonged exposure to chloride environments such as seawater, further oxidation processes occur, leading to the formation of copper (II) compounds[8]. For example, cupric hydroxychloride [$Cu_2(OH)_3Cl$] and cupric oxide (CuO) have been found in significant amounts under certain conditions[9],

$$Cu_2O(s) + 2H_2O(l) + Cl^{-}(aq) \rightarrow Cu_2(OH)_3Cl(s) + H^{+}(aq) + 2e^{-} \quad (5)$$

Mansfeld *et al.*[7] reported that the Atacamite is much less protective than cuprous oxide (Cu_2O) in marine environments.

The incidence of failures of aluminium brass heat exchanger tubes and copper nickel iron seawater pipes occurring after only a short service time have been alarming. These have been associated with the presence of sulphide films on the alloy surfaces as a result of a polluted seawater environment. Extensive research has shown that corrosion is particularly aggressive in polluted harbours and estuaries, where the ebb and flow of tides cause a change from polluted anaerobic to relatively fresh aerated seawater[10-15]. When transferring from a polluted to a non-polluted environment, the sulphide and the oxygen can co-exist for a short period. These studies showed that accelerated attack is not caused by the presence of sulphide alone but when sulphide and oxygen contact the metal surface simultaneously.

Syrett[11] has suggested that the sulphide ion (or sulphide oxidation products) can

interfere with the normal growth of the protective oxide film that forms on the surface of copper nickel alloys exposed to seawater. The result is the production of a porous, non-protective cuprous sulphide film, which interferes with the normal passivation of the alloy when exposed to unpolluted aerated seawater. According to Sanchez and Schiffrin[16] the main effect of the pollutant is to drastically increase the rate of the oxygen reduction reaction, while the anodic process remains largely unaltered.

A proposed corrosion mechanism for copper nickel alloys in sulphide polluted waters is given below[17]. The cathodic reaction in deaerated seawater,

$$2H^{+}_{(aq)} + 2e^{-} \rightarrow H_{2(g)} \quad (6)$$

or in aerated seawater

$$O_{2(g)} + 2H_2O_{(l)} + 4e^{-} \rightarrow 4OH^{-}_{(aq)} \quad (1)$$

can be accompanied by,

$$Cu\text{-}Ni_{(s)} + HS^{-}_{(aq)} \rightarrow Cu\text{-}Ni(HS^{-})_{ads} \quad (7)$$

$$Cu(HS^{-})_{ads} \rightarrow Cu(HS)_{(s)} + e^{-} \quad (8)$$

$$Ni(HS^{-})_{ads} \rightarrow Ni(HS)^{+}_{(aq)} + 2e^{-} \quad (9)$$

$$Cu(HS)_{(s)} \rightarrow Cu^{+}_{(aq)} + HS^{-}_{(aq)} \quad (10)$$

$$Ni(SH)^{+}_{(aq)} \rightarrow Ni^{2+}_{(aq)} + HS^{-}_{(aq)} \quad (11)$$

The reaction of Cu^{+} and Ni^{2+} ions with HS^{-} can produce copper and nickel sulphides, which are insoluble and precipitate on the alloy surface,

$$2Cu^{+}_{(aq)} + HS^{-}_{(aq)} + OH^{-}_{(aq)} \rightarrow Cu_2S_{(s)} + H_2O_{(l)} \quad (12)$$

$$Ni^{2+}_{(aq)} + HS^{-}_{(aq)} + OH^{-}_{(aq)} \rightarrow NiS_{(s)} + H_2O_{(l)}. \quad (13)$$

At the pH of seawater (8-8.2), the sulphide ion is not stable and the hydrosulphide ion is preferred,

$$S^{2-}(aq) + H_2O(l) \rightarrow HS^-(aq) + OH^-(aq) \quad (14)$$

The OH^- ions produced increase the local pH at the electrode surface and form insoluble hydroxides,

$$Cu^+(aq) + OH^-(aq) \rightarrow Cu(OH)(s) \quad (15)$$

$$Ni^{2+}(aq) + 2OH^-(aq) \rightarrow Ni(OH)_2(s) \quad (16)$$

The corrosion products tend to be a brittle, non-adherent and non-protective mixture of hydroxides and sulphides of copper and nickel.

In the present work, the oxygen reduction reaction on copper and MARINEL™ in sulphide contaminated and in uncontaminated sodium chloride solutions has been investigated using a rotating disc electrode. An emerging technique, atomic force microscopy has been used to study the initiation of the corrosion process of copper and its alloy, and also to correlate the influence of passive layers on the corrosion reaction.

2. EXPERIMENTAL DETAILS

2.1 Materials

Copper metal, 99.9% pure, was supplied by Goodfellow Metals. MARINEL™, the wrought and precipitate hardened copper nickel, was obtained from Langley Alloys in rod form. Its composition is given in Table 1.

Table 1 Composition of MARINEL™

Element	Mn	Ni	Cu	Al	Nb	Fe	Pb
wt %	4.57	19.1	71.93	1.9	0.72	1.18	0.60

2.2 Electrochemical investigations

Electrochemical measurements were made using an EG&G model 636 rotating disc electrode system coupled to an EG&G Princeton Applied Research 273A Potentiostat/Galvanostat, or an ACM potentiostat and an ACM S300 sweep generator with the current *versus* potential output recorded on a Philips PM 8271 XYt chart recorder. The rotating disc electrode (RDE) consisted of a copper or copper nickel alloy disc of 0.2 cm radius, set in an insulated PTFE shroud of radius 0.6 cm. The experiments were carried out in a three compartment glass cell with the counter electrode (platinum gauze) separated from the working electrode by a Nafion™ cation exchange membrane. All electrode potentials were measured with respect to a saturated calomel electrode (Radiometer K410). The pH of the solutions was monitored using a Jenway 3420 electrochemistry analyser.

The RDEs were polished with a 0.3 μm Al_2O_3/water slurry. Prior to each polarisation measurement the sodium chloride solutions were aerated for 5 min to produce an air saturated electrolyte. The rest potential of the working electrode was measured with respect to the SCE, and then the potential was linearly scanned approximately 1000 mV in the negative direction. For the diffusion coefficient measurements, polarisation curves were obtained for rotation rates ranging from 250 to 2000 rev min^{-1} at a potential sweep rate of 2 mV s^{-1} to maintain steady state conditions.

2.3 Atomic force microscopy

Images were obtained in the contact mode with a Discoverer TMX 2010 Atomic Force Microscope (Topometrix Corporation, Santa Clara, California, USA); the force constant was 0.012 nN.

The copper nickel alloy was cut into 10 mm diameter, 2 mm thick discs. The samples were polished with an 0.3 μm alumina/water slurry, washed with double distilled water and finally rinsed with absolute alcohol. The air-dried samples were placed in the solutions of interest for varying time intervals after which they were removed, dried in air and observed directly.

3. RESULTS AND DISCUSSION

3.1 Electrochemical investigations

Figures 1a-b show polarisation curves for oxygen reduction, equation (1), on copper and copper nickel in aerated, 3% sodium chloride solution (pH = 6.2 and 293 K). In both cases, well-defined plateau regions, due to convective diffusion limited oxygen reduction, are observed. These extend from -650 to -1150 mV (vs.SCE), at which point the onset of the hydrogen evolution reaction can be observed.

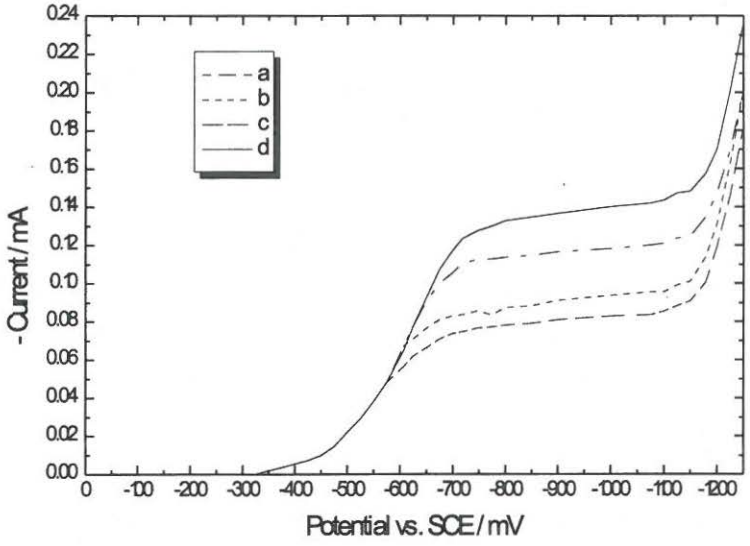

Figure 1a *Current-potential curves for the reduction of oxygen in aerated 3% sodium chloride solution at a copper RDE. Rotation rates were (a) 500, (b) 750, (c) 1250 and (d) 1750 rpm. WE: copper disc, RE: SCE and CE: Platinum. Potential sweep rate 2 mV s^{-1}, pH = 6.2 and T = 293 K.*

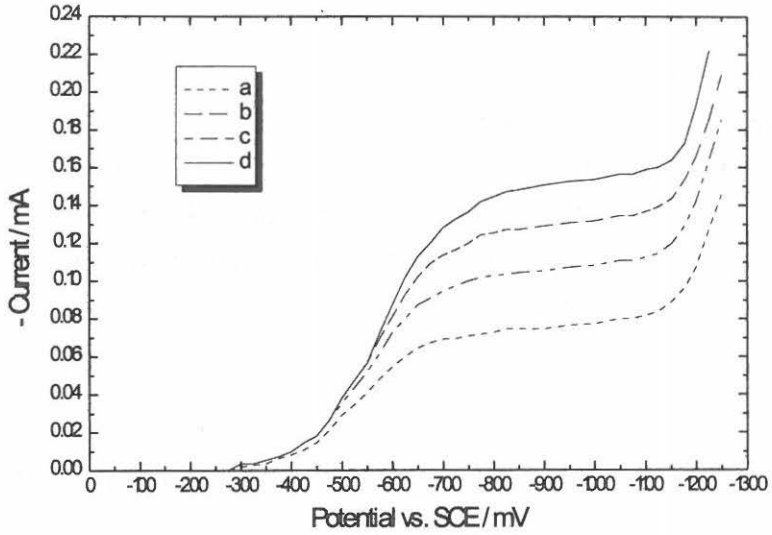

Figure 1b *Current-potential curves for the reduction of oxygen in aerated 3% sodium chloride solution at a copper nickel RDE. Rotation rates were (a) 500, (b) 1000, (c) 1500 and (d) 2000 rpm. WE: copper nickel disc, RE: SCE and CE: Platinum. Potential sweep rate 2 mV s^{-1}, pH = 6.2 and T = 293 K.*

Figures 2a-b show the corresponding cathodic polarisation curves in the presence of 5 ppm sodium sulphide (pH 7.2 and 293 K). A second limiting current region extending from -480 to -850 mV (SCE) is observed for both copper and copper nickel. However this second plateau is less well defined on the alloy surface.

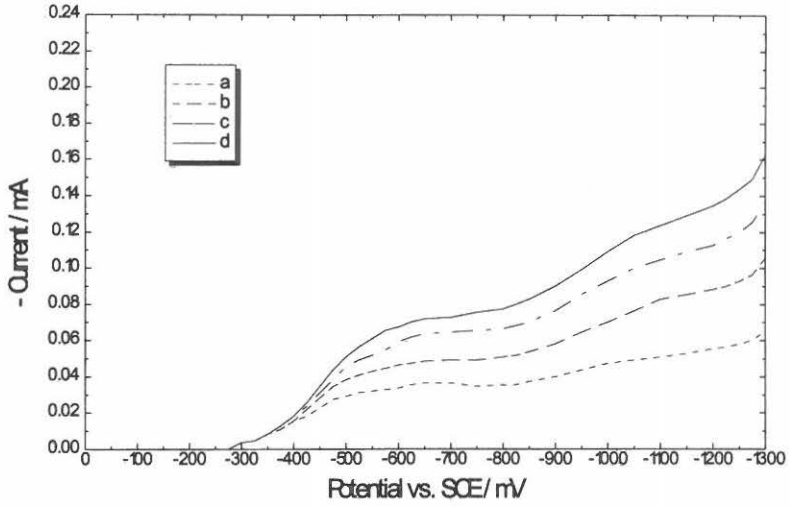

Figure 2a *Current-potential curves for the reduction of oxygen in aerated 3% sodium chloride containing 5 ppm sodium sulphide, solution at a copper RDE. Rotation rates were (a) 250, (b) 750, (c) 1250 and (d) 1750 rpm. WE: copper disc, RE: SCE and CE: Platinum. Potential sweep rate 2 mV s^{-1}, pH = 7.2 and T = 293 K.*

Levich plots of limiting current *versus* the square root of the rotation rate (Figure 3) were linear, showing the oxygen reduction reaction to be mass transport controlled. From this data, the diffusion coefficient for oxygen reduction at the RDE under steady state conditions was calculated *via* the Levich equation (17).

$$I_L = 0.62\, n\, F\, A\, D^{2/3}\, \nu^{-1/6}\, \omega^{1/2}\, c_B \qquad (17)$$

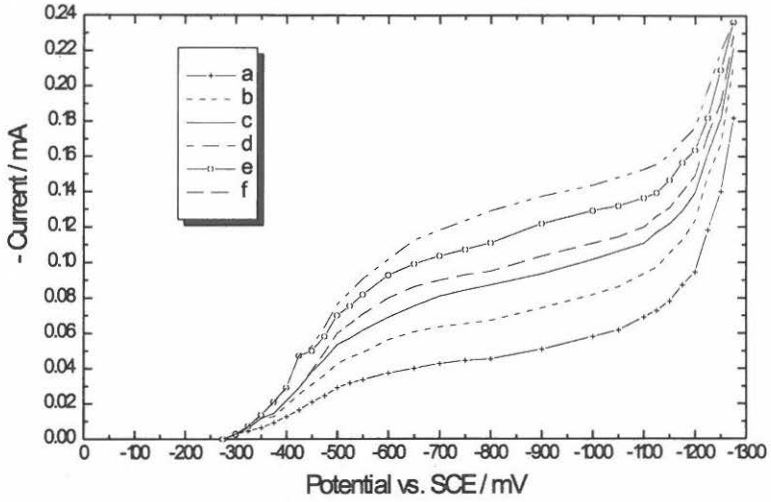

Figure 2b *Current-potential curves for the reduction of oxygen in aerated 3% sodium chloride containing 5 ppm sodium sulphide, solution at a copper nickel RDE. Rotation rates were (a) 500, (b) 1000, (c) 1250, (d) 1500, (e) 1750 and (f) 2000 rpm. WE: copper nickel disc, RE: SCE and CE: Platinum. Potential sweep rate 2 mV s^{-1}. The pH was 7.2 and T = 293 ± 2 K.*

Assuming the cathodic reaction is the reduction of oxygen, (n = 4) and the bulk concentration of oxygen (c_B) is 2.0 x 10^{-4} mol dm^{-3} [18], the diffusion coefficients for oxygen reduction on copper nickel and copper rotating disc electrodes were calculated to be 1.50 x 10^{-5} cm^2 s^{-1} and 1.44 x 10^{-5} cm^2 s^{-1}, respectively. These values compare favourably with those of 1.4 x 10^{-5} cm^2 s^{-1} obtained by Wood *et al.* [19] for 70/30 copper nickel, (B.S.2875), and 1.7 x 10^{-5} cm^2 s^{-1} for aluminium brass in natural seawater[16].

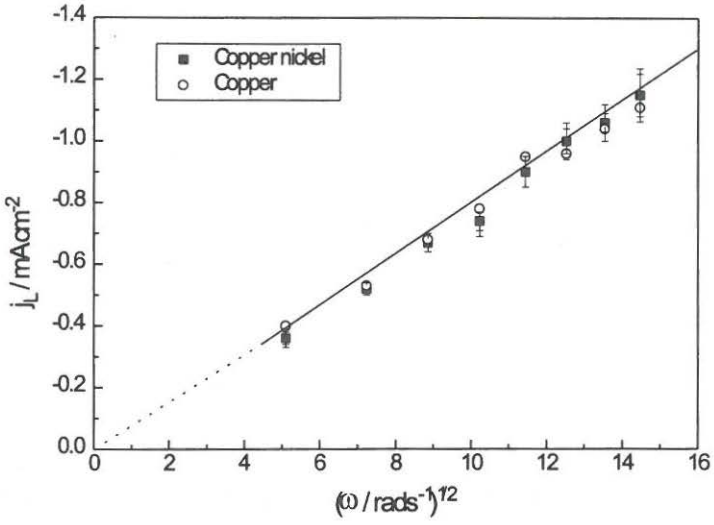

Figure 3 *Levich plots for copper and copper nickel RDEs in aerated 3% sodium chloride at pH = 6.2 and 293 K.*

Levich plots for the copper nickel and copper in aerated 3% sodium chloride solutions containing 5 ppm sodium sulphide are shown in Figures 4 and 5, where slope (b) represents the limiting current plateau between -480 and -850 mV. The values of the diffusion coefficients for oxygen reduction, slope (a), were slightly reduced to 1.35 x 10^{-5} and 1.24 x 10^{-5} cm^2 s^{-1} for the copper nickel and copper respectively. This may result from the reaction of sulphide with the dissolved oxygen as proposed by Beccaria *et al.* [20]. The chemistry of aqueous sulphides and oxidation products is extremely complex but available data indicates that dissolved sulphide is oxidised fairly rapidly in both sodium chloride and seawater solutions. Ostlund and Alexander[21] showed that for air saturated seawater with a sulphide concentration of 3.8 ppm, the half-life of the sulphide was of the order of 20 min. Avrahami *et al.*[22], in a detailed mechanistic study of this reaction, showed that elemental sulphur, sulphite (SO_3^{2-}), sulphate (SO_4^{2-}) and thiosulphate ($S_2O_3^{2-}$) are formed and that the oxidation of sulphur to the oxyanions is slow. Also sulphides may be oxidised by dissolved oxygen to a variety of polysulphides.

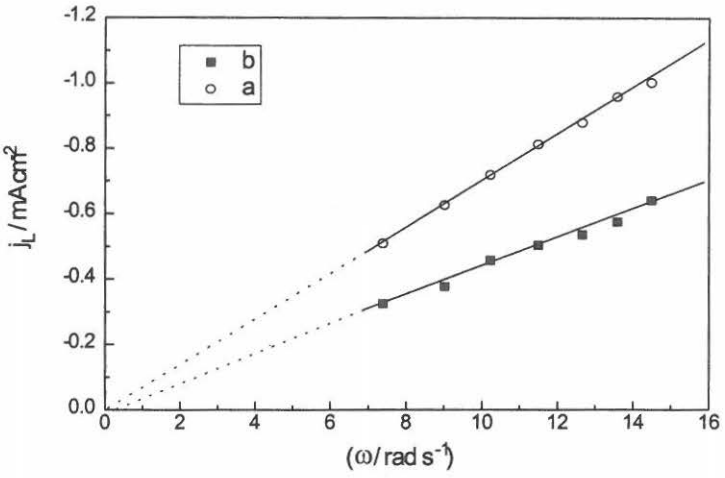

Figure 4 *Levich plots for a copper RDE in aerated 3% NaCl + 5 ppm Na_2S at pH 7.2 and 293 K. (a) Represents oxygen reduction plateau at -650 to -1150 mV and (b) the additional plateau at -480 extending to -850 mV.*

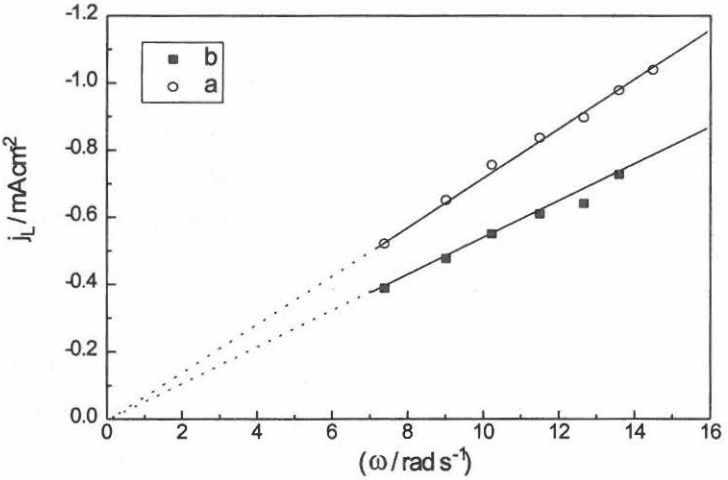

Figure 5 *Levich plots for a copper nickel RDE in aerated 3% NaCl containing 5 ppm Na_2S, pH 7.2, 293 K. (a) represents oxygen reduction plateau at -650 to -1150 mV and (b) the additional plateau at -480 extending to -850 mV.*

The magnitude of the slope for the second plateau region is smaller than that for the reaction (1). It is possible that it is due to the production of hydrogen peroxide[23],

$$O_{2(g)} + 2H_2O_{(l)} + 2e^- \rightarrow H_2O_{2(aq)} + 2OH^-_{(aq)} \quad (18)$$

$$H_2O_{2(aq)} + 2e^- \rightarrow 2OH^-_{(aq)}. \quad (19)$$

The additional peaks observed in the presence of sulphide ions can be explained by a mechanism involving oxygen reduction on two types of surface sites with different reactivities[23].

It has been reported that the more catalytic surface is comprised of Cu(0) and Cu(I) sites, where the Cu(I) species is stabilised as $Cu(OH)_{ads}$ and/or submonolayer Cu_2O. The less catalytic site consists of Cu(0) only. Oxygen reduction is believed to proceed by a series pathway involving an adsorbed peroxide intermediate on both sites. The majority of the peroxide is reduced prior to desorption at Cu(0) sites. However, some is released before being reduced at Cu(0)/Cu(I) sites, hence, the presence of the additional peak at -400 mV *vs.* SCE.

This was confirmed by the results of King *et al.*[23] who studied the oxygen reduction on copper in neutral sodium chloride (1 mol dm^{-3}, T= 296±3 K) using a rotating ring disc electrode. They found that the extent of the surface coverage by the catalytic species was favoured by a higher interfacial pH, which is in turn favoured by a higher electrolyte pH. In the presence of sulphide, the electrolyte pH increases from a slightly acidic pH 6.2 to 7.2.

They derived a scheme for oxygen reduction on the two types of copper surface sites. The less catalytic surface site was designated S_A and here the oxygen reduction proceeded with no change in the oxidation state of the Cu(0) species. They proposed that the reaction proceeds via the adsorption of a peroxide (HO_2^-) intermediate on the surface, which is reduced prior to desorption as in shown in equation (20).

$$S_A + O_2 \xrightarrow{+e} S_A\text{-}O_{2(ads)} \xrightarrow{+e+H^+} S_A\text{-}HO_2^-{}_{(ads)} \rightarrow S_A + 4OH^- \quad (20)$$

$$S_B + O_2 \xrightarrow{+e} S_B\text{-}O_{2(ads)} \xrightarrow{+H^+} S^+{}_B\text{-}O_2^-{}_{(ads)} \xrightarrow{+e} S_B\text{-}O_2^-{}_{(ads)} \rightarrow S^+{}_B\text{-}HO_2^-{}_{(ads)} \rightarrow \begin{cases} HO_2^-{}_{(bulk)} \\ S_B + 4OH^- \end{cases} \quad (21)$$

where S_A = Cu(0) (less catalytic) and S_B = Cu(0)/Cu(I) (catalytic). The more catalytic site S_B exists as either Cu(0) or Cu(I) species. The Cu(I) surface site is stabilised by the adsorption of OH^- (or Cl^-) or as a submonolayer Cu_2O. Oxygen reduction proceeds via electron relay between Cu(0)/Cu(I) sites and adsorbed oxygen species. Unlike S_A sites, the rate of reduction of the peroxide does not greatly exceed the rate of desorption and some peroxide is released into solution. The percentage surface coverage by the two types of site is determined by the interfacial and electrolyte pH and potential. Higher interfacial values (and higher bulk pH) favour the formation of the more catalytic site. The results of the present study are consistent with this theory as no additional peroxide peak was produced in the absence of sulphide where a more acidic pH of 6.2 exists.

The theory is further supported by calculating the number of electrons involved in the two reduction processes on the copper and copper nickel via the Levich equation (utilising the diffusion coefficients determined in the absence of sulphide). For copper, the number of electrons involved changes from 2.3 to 3.8, effectively 2 to 4. For the copper nickel, the change is from 2.9 to 3.8 effectively 3 to 4. Hence, the intermediate formation of peroxide, reaction (18), is the two electron process producing the additional plateau. If the peroxide intermediate is strongly adsorbed (and reaction (19) is fast) prior to desorption, the reduction of oxygen is a 4 electron process. However, if it is not strongly adsorbed, the stoichiometry will depend on the diffusional conditions imposed[19]. Thus, the total number of electrons involved alters from 4 to 2 as the flow velocity increases and less peroxide is reduced. Hence, the second plateau becomes more prominent at higher rotation rates of a disc electrode.

3.2 Atomic force microscopy investigations

It has been stated that the protective corrosion products form within minutes or even seconds on freshly polished copper nickel alloys[11]. To investigate this, atomic force microscopy was used to study the morphology and rate of film formation on copper nickel after exposure to aerated 3% sodium chloride and sodium sulphide contaminated solutions.

Figure 6 shows an *ex situ* AFM image of the unexposed copper nickel surface. Scratch marks from the polishing process and particles of the alumina itself can be clearly seen on the sample surface. Subsequent investigations showed that the alumina did not interfere or contribute to the surface film formation as there was no correlation between the location of the corrosion product nucleation sites and the alumina present. However, to avoid any possible problems, later samples were sonicated prior to exposure to the relevant electrolyte.

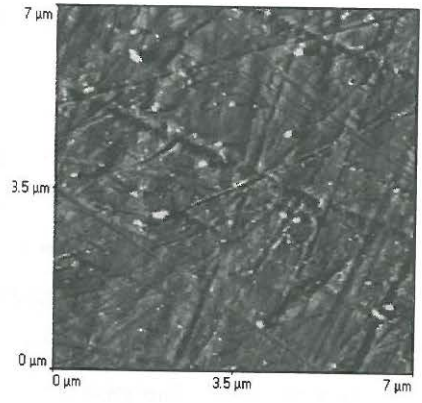

Figure 6 *Atomic force microscopy image of polished copper nickel alloy showing traces of alumina on the metal surface.*

Film formation on the copper nickel alloy in aerated 3% sodium chloride solution, as seen in Figures 7a and b, was rapid. After a 5 minute exposure to the solution, a particulate film is evident covering the majority of the sample surface with only one polished area remaining visible. However, this region was obscured after 60 minutes when the surface

of the copper nickel alloy was seen to be completely covered with a uniform layer.

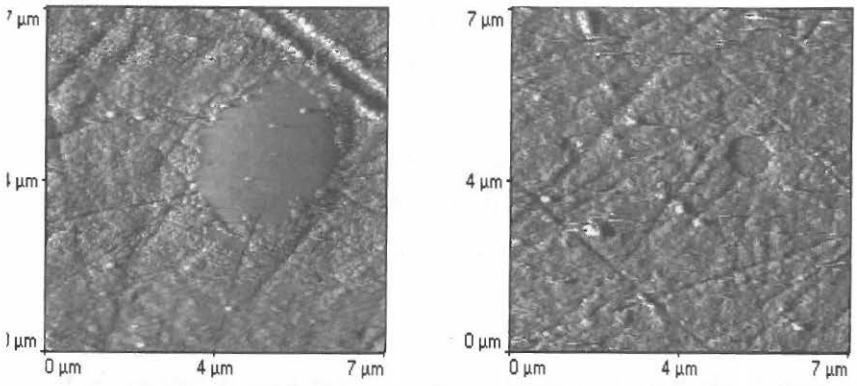

(a) (b)

Figure 7 *Copper nickel exposed to aerated 3% sodium chloride solution for (a) 5 minutes and (b) 60 minutes.*

Line profiles of the unfilmed area in Figure 7a showed it to be a convex protrusion from the surface. This suggests that it is most likely to be a precipitate known to form in aluminium age hardened copper nickels. Such micron scale features ranging from 0.1 to 3 µm diameter have been found in MARINEL™ which analysis has confirmed as Ni_3Al, Ni_3Nb, $Ni_{16}NbSi_9$ and (more commonly) orthorhombic Ni-Nb-Si-Fe intermetallic phases[24]. It is feasible that these particles interfere with normal film growth. Scanning electron microscopy coupled with energy dispersive analysis of the sample proved inconclusive, as this is a *near* surface technique and the electron beam can penetrate the surface to depths of approximately 1 µm[25].

In the presence of 5 ppm sulphide, a uniform film formed on the copper nickel sample after 5 minutes exposure, Figures 8a-b. This suggests more rapid film formation in the presence of sulphide ions. In both solutions, the films continued to grow with time as indicated by the disappearance of the scratch marks originally present from the polishing process.

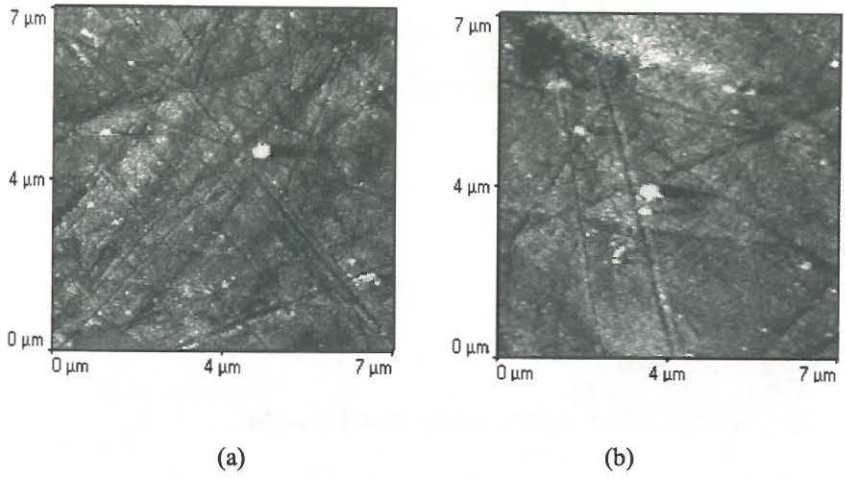

Figure 8 *Copper nickel exposed to aerated 3% sodium chloride solution containing 5 ppm sodium sulphide for (a) 5 minutes and (b) 60 minutes.*

These results agree with the proposal that within the first few seconds of exposure to sulphide polluted seawater, when the corrosion potential still exceeds *ca.* -260 mV (vs.SCE), a thin film or sub-layer forms on the metal surface (deduced from scanning electron microscopy and X-ray diffraction data) [11]. This film, termed the oxide-type-layer (Figure 9), is thought to be predominately cuprous oxide doped with the alloying elements (Ni, Fe and possibly Mn). Due to the composition and microstructural variations at grain boundaries, the oxide does not grow as fast at these locations, therefore, these boundaries appear as cracks in the corrosion product.

The typical alloy grain size in the copper nickel, shown in Figure 10, ranges from approximately 40 μm^2 to 100 μm^2, which is much larger than the scan range (7 µm × 7 µm) of the AFM micrographs shown. Therefore, it is reasonable to assume that the AFM images show the growth of the particulate layers on top of such a sub layer, as shown in Figure 9.

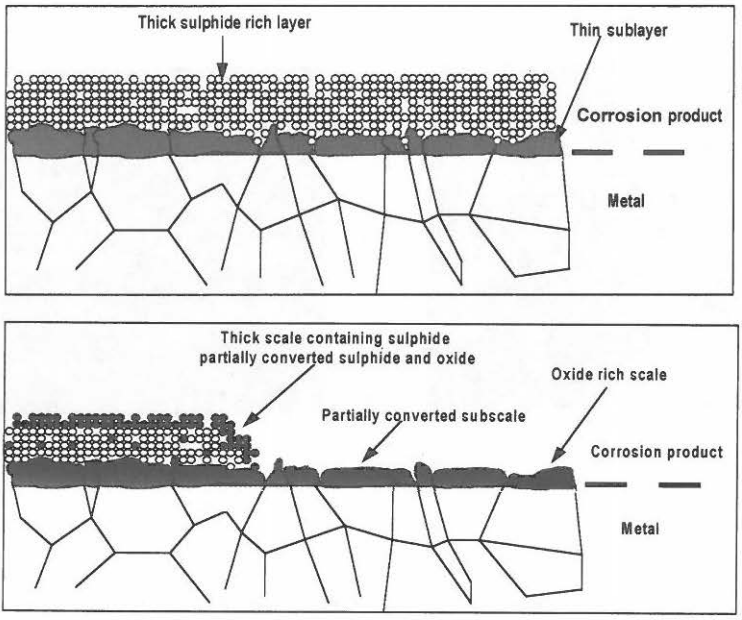

Figure 9 *Schematic diagrams showing the corrosion products resulting from exposure to (a) sulphide polluted seawater and (b) sulphide polluted deaerated seawater then aerated clean seawater*[11].

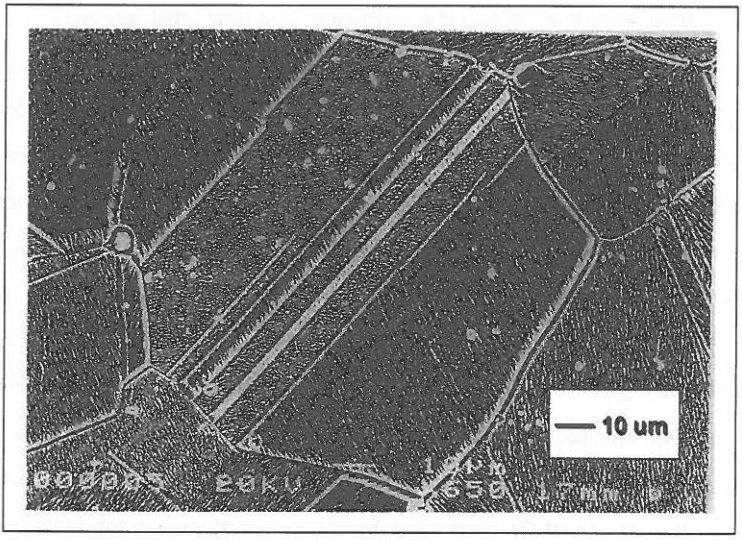

Figure 10 *Scanning electron micrograph of ferric chloride etched MARINEL™ showing the alloy grain boundaries.*

The images shown in Figure 11 show that the particulate sizes of the layers formed on the samples, varied for the contaminated and uncontaminated solutions. This can be clearly seen by the topographic analyses in Figures 12 and 13.

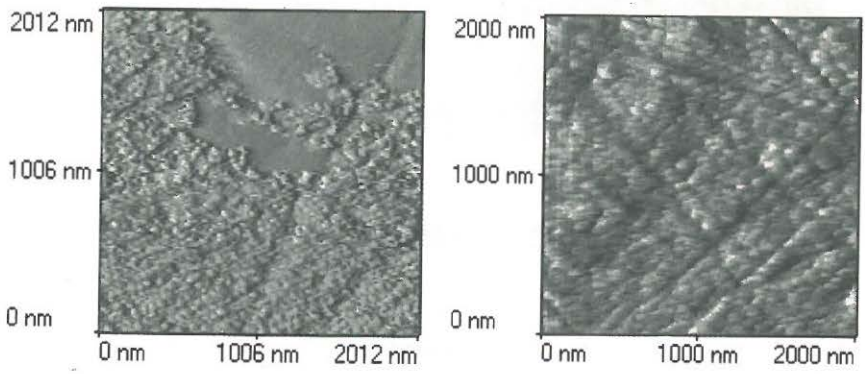

(a) (b)

Figure 11 *Copper nickel exposed to (a) uncontaminated and (b) contaminated (with 5 ppm sodium sulphide) 3% sodium chloride solution (aerated) for 5 minutes.*

The particulates formed in both solutions appear to have a "granular" type structure. In the presence of sulphide pollution, the average film particle size was 300 nm in diameter, compared to 68 nm for the sulphide-free sea water. However, similar particle heights of 6 nm were observed for both types of particulates.

The increase in the particle size of the surface films could account for the well-documented increase in porosity[10-15] of the film towards the corrosive environment, hence reducing its corrosion resistance.

This result is somewhat unexpected as according to the theory of oxidation, the film formed in the presence of sulphide contamination should be more protective. However, this does not account for the more defective structure of metal sulphides, film spalling and the enhanced cathodic reduction reaction occurring on the sulphide layer, resulting in the pitting corrosion[26]. The oxidative description of protective film formation

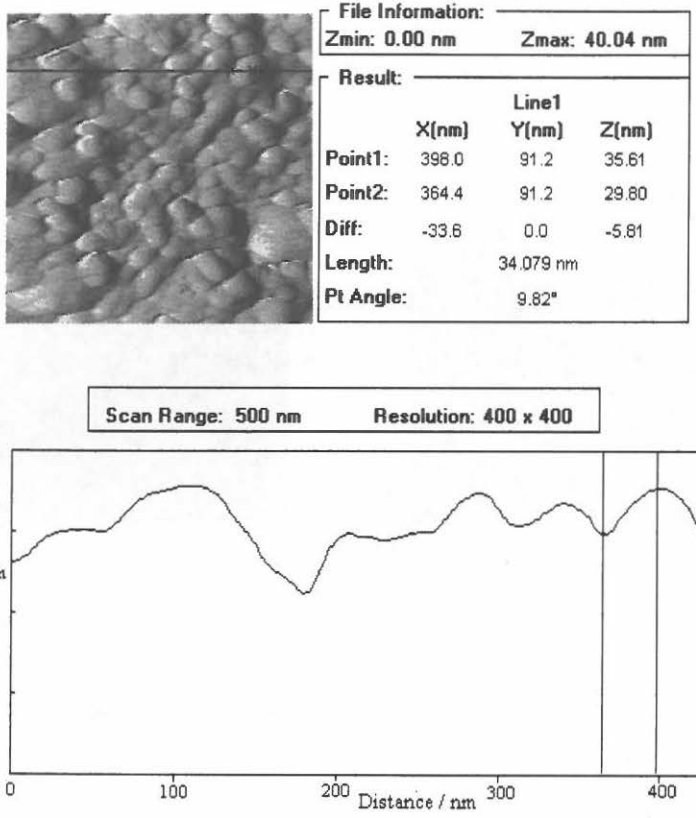

Figure 12 *Topographic analysis of copper nickel exposed to aerated 3% sodium chloride for 5 minutes.*

suggests an eventual parabolic corrosion rate governed by diffusion of a cation *via* vacancies, which rather implies lattice diffusion. This is obviously an oversimplification. The films formed consist of grains and preferential diffusion down grain boundaries may be a major feature of the growth process. Such mechanisms place great emphasis upon the microstructure of the oxide particularly the grain size. It could be assumed, therefore, that the finer grains formed in the unpolluted solution would result in a relatively high density of grain boundary paths for oxide growth when compared to the film formed in sulphide contaminated solution.

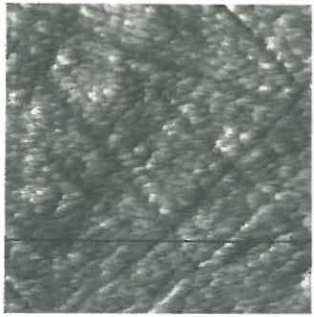

File Information:
Zmin: 0.00 nm Zmax: 47.82 nm

Result:

	Line1			Line2		
	X(nm)	Y(nm)	Z(nm)	X(nm)	Y(nm)	Z(nm)
Point1:	1872.5	1515.0	30.24	1872.5	1515.0	30.24
Point2:	1726.4	1515.0	23.97	1726.4	1515.0	23.97
Diff:	-146.2	0.0	-6.27	-146.2	0.0	-6.27
Length:		146.303 nm			146.303 nm	
Pt Angle		2.46°			2.46°	

Scan Range: 2000 nm Resolution: 400 x 400

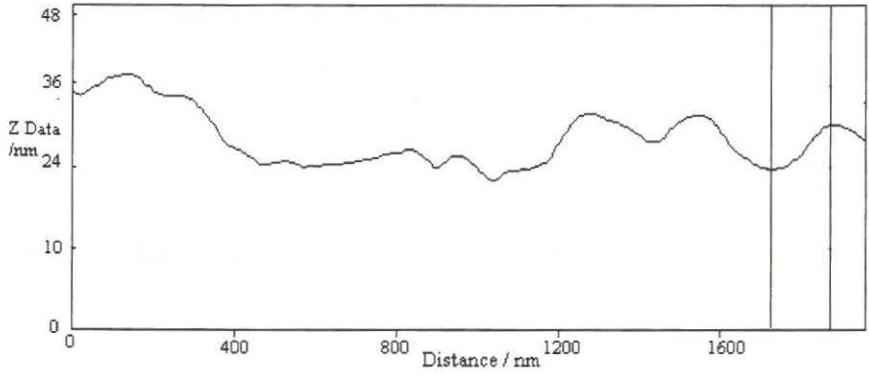

Figure 13 *Topographic analysis of copper nickel surface exposed to aerated 3% sodium chloride containing 5 ppm sodium sulphide for 5 minutes.*

4. CONCLUSIONS

Electrochemical studies of copper and MARINEL™ in seawater show that the limiting current for oxygen reduction at both electrodes is mass transfer controlled, due to the rate of convective diffusion of dissolved oxygen. The reaction itself is similar on both copper nickel and copper substrates with comparative limiting currents at potentials of -650 to -1150 mV (vs.SCE) from which diffusion coefficients of 1.50×10^{-5} and 1.44×10^{-5} $cm^2 s^{-1}$ respectively may be calculated. In the presence of sulphide ions, a second mass transport

limited cathodic reaction, attributed to the formation of hydrogen peroxide/ hydroxide ions, is observed. This proposal is supported by the increased solution pH in the presence of the sulphides.

AFM studies indicate that particulate film formation on copper nickel occurs within about 5 minutes in both sulphide contaminated and pure sodium chloride solutions. Film-free dome shaped protrusions, present after exposure to uncontaminated conditions, are thought to be precipitates present in the copper nickel. The heights of the particles formed in the sodium chloride and sulphide contaminated solutions are comparable at approximately 6 nm. However the particle diameters are much larger (300 compared to 68 nm) in the presence of sulphide.

Further work should focus on spectroscopic investigations to confirm the nature of the products formed at the more negative potentials as well as on *in situ* AFM experiments to follow the very early stages of film formation in a variety of corrosive media.

Acknowledgements

The authors would like to thank the MTD for the EPSRC studentship and Langley Alloys for financial support.

References

1. C. A. Clark, S.Driscoll and P. Guha, *British Corrosion Journal*, 1992, **27**, 157.
2. G. Bianchi, G. Fiori, P. Longhi and F. Mazza, *Corrosion*, 1978, **34**, 396.
3. A.H. Tuthill, *Materials Performance*, 1987, **12**, 12.
4. R.F. North and M.J. Pryor, *Corrosion Science*, 1970, **10**, 297.
5. J..M.Popplewell, R. J. Hart and J. A. Ford, *Corrosion Science*, 1973, **13**, 295.
6. C. Kato, J. E. Castle, B. G. Ateya and H. W. Pickering, *J.Electrochem.Soc.*, 1980, **127**, 1897.
7. F. Mansfeld, G.Liu, H. Xiao, C.H Tsai and B.J Little, *Corrosion*, 1994, **36**, 2064.
8. S. R.de Sanchez, *J. Electroanal. Chem.*, 1991, **307**, 73.
9. J. Kruger, *J.Electrochem.Soc.*, 1961, **108**, 503.

10. J. F. Bates and J. M Popplewell, *Corrosion NACE*, 1975, **31** No 8, 269.
11. B. C. Syrett, *Corrosion Science*, 1981, **21**, 187.
12. B. C. Syrett, D. D. Macdonald and S.S.Wing, *Corrosion, NACE*, 1979, **35**, 409.
13. L.E Eiselstein, B.C Syrett, S.S. Wing and D.Caligiuri, *Corrosion Science*, 1983, **23**, 223.
14. B.C Syrett, *Corrosion NACE*, 1977, **23**, 257.
15. J.P. Gudas and H.P Hack, *Corrosion NACE*, 1979, **35**, 67.
16. S.R. de Sanchez and D.J Schiffrin, *Corrosion Science*, 1982, **22**, 597.
17. M.R.Reda and N.Alhajji, *Br. Corr. J.*, 1995, **30** No.1, 58.
18. M. Stratmann and J. Muller, *Corrosion Science*, 1994, **36**, 327.
19. R.J.K. Wood, S.P. Hutton and D.J.Schiffrin, *Corrosion Science*, 1990, **30**, 1199.
20. A.M.Beccaria, G. Poggi, P. Traverso and M. Ghiazza, *Corrosion Science*, 1991, **32**, 1267.
21. H. G. Ostlund and J. Alexander, *J. Geophys. Res.*, 1963, **68**, 3995.
22. M. Avrahami and R.M. Golding, *J. Chem. Soc.*, (1968), 647.
23. F.King, M.J.Quinn and C.D Litke, *J. Electroanal. Chem.*, 1995, **385**, 45.
24. C.D.S Tuck, K.C. Bendall, G.J.W. Radford, S.A Campbell, F.C. Walsh and R.J. Grylls, NACE International Annual Conferrence Proceedings, 1996.
25. R. Baboian, Corrosion Tests and Standards, Application and Interpretation, ASTM Manual Series, 1995,
26. G.J.W. Radford, The Marine Corrosion and Electrochemical Characteristics of MARINEL Copper Nickel Alloy, PhD Thesis, (1998), 235.